Electronic Supplementary Material (ESI) for Analyst

Supplementary Information for **"Desorption Electro-Flow Focusing Ionization of Explosives and Narcotics for Ambient Pressure Mass Spectrometry"**

Thomas P. Forbes, Tim M. Brewer, and Greg Gillen
National Institute of Standards and Technology, Gaithersburg, MD, USA

Secondary Droplet Current Measurements

We measured the secondary droplet current, transmitted from the DEFFI source, as a function a couple system parameters, i.e., focused flow rate (Figure S2), focusing gas pressure (Figure S3), and applied potential (Figure S2). The time dependent current measured for a deflected DEFFI spray off of a plain glass slide demonstrated a sharp spike in current as the potential was initially applied, followed by an exponential decay to a stabilized steady state current (Figure S1). Similar capacitive charging behavior was reported for DESI.[1] The experimental currents reported were taken from an average over the steady state region of the deflected current response for a given set of DEFFI parameters. All data points and error bars represent the average values and standard uncertainty (represented by the standard deviation), respectively, for steady state currents obtained from 3 to 5 experiments. Additional details of the charge transmission characteristics of desorption electro-flow focusing have been investigated elsewhere.[2]

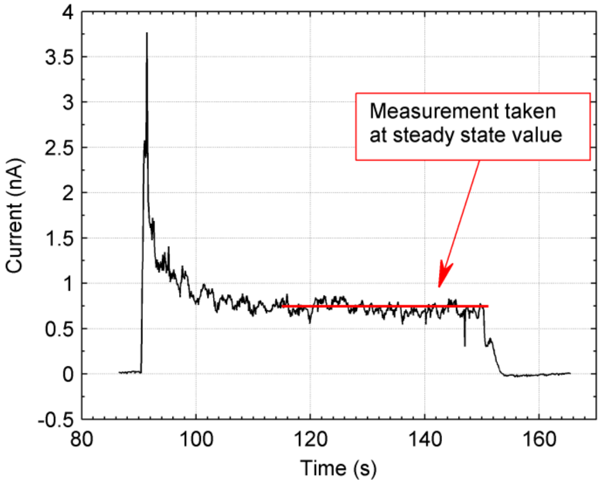

Figure S1. Representative example of the experimentally measured current time response. All data points were taken at the steady state value of each set of conditions.

Figure S2 demonstrates the expected increase in current with increasing potential and increasing solvent flow rate. Details of the asymptotic behavior of the secondary droplet current can be found elsewhere.[2]

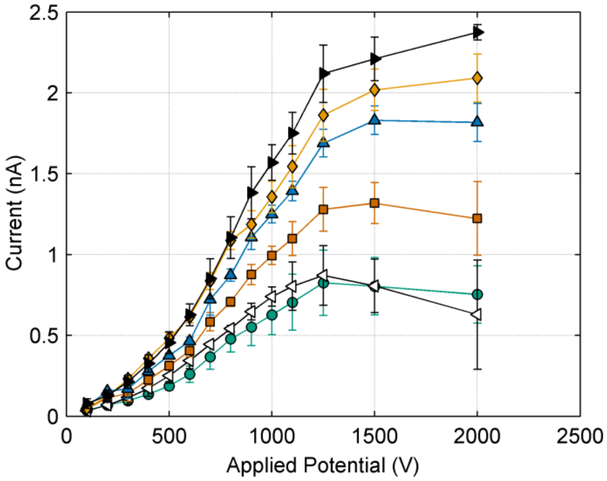

Figure S2. Experimentally measured secondary droplet current for a 50 % volume fraction of methanol solution in water sprayed onto a glass slide as a function of applied potential for a 50° angle, 10 psi focusing gas pressure, and 3 µl/min (-●-), 4 µL/min (-◅-), 5 µL/min (-■-), 5.75 µL/min (-▲-), 6.5 µL/min (-◆-), and 8 µL/min (-►-) flow rates. Data points and uncertainty expressed as the average values and standard deviations, respectively, for steady state currents obtained from 3 to 5 experiments.

Figure S3 shows the measured deflected current of DEFFI at 1kV applied potential as a function of the flow focusing gas pressure in the range of approximately 6.5 kPa to approximately 70 kPa (1 psi to 10 psi) for a number of focused fluid flow rates. For the flow rates investigated, DEFFI produced an elevated current at low focusing gas pressures that decreased, reached a minimum and then increased again. From direct visualization of the DEFFI jet and spray using backlighting and prior results in the literature on reflective electrospray ionization (RESI),[3] we found that at low focusing gas pressures there was insufficient pneumatic mechanical force on the droplet stream to direct the highly charged droplets onto the intermediate sample substrate. In this case, the highly charged droplets were electrostatically forced directly from the DEFFI source to the collecting electrode by the external electric field without contacting the sample surface. It is important to note that for desorption-based MS analyses, where the sample analyte is desorbed from an intermediate substrate surface, these droplets/ions will not contribute to the analyte's MS signal. As the focusing gas pressure increased, the force directing the jet toward the sample surface increased, effectively decreasing the portion of drops transported directly to the collecting electrode and therefore the overall measured current. This trend continued until a minimum was reached. Increasing the focusing gas pressure above this minimum increased the measured current in the range investigated. Based on these results, the DEFFI source was operated at 68.95 kPa (10 psi) focusing gas pressure for all remaining experiments reported here. While, electro-flow focusing and DEFFI are operational at much higher applied pressures, the focus of this work is the low pressure regime.

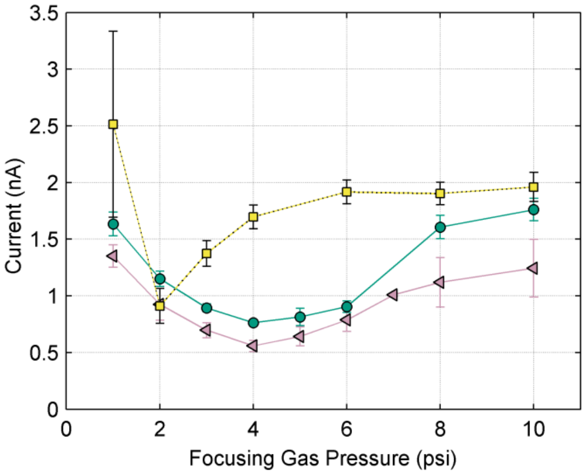

Figure S3. Experimentally measured current for a 50 % volume fraction of methanol in water deflected off of a glass slide as a function of focusing gas pressures for DEFFI at a 45° angle, 1 kV applied potential, and 3 µL/min (-◀-), 5 µL/min (-●-), and 8 µL/min (-■-) flow rates. Data points and uncertainty expressed as the average values and standard deviations, respectively, for steady state currents obtained from 3 to 5 experiments.

Additional Negative Ion DEFFI Mass Spectra and Analysis

Here, we provide additional analysis of various explosives, including, 2,4,6-trinitrotoluene (TNT), cyclotrimethylenetrinitramine (RDX), and pentaerythritol tetranitrate (PETN), in negative ion mode DEFFI-MS. Mass spectra for TNT (Figure S4), RDX (Figure S6), and PETN (Figure S8) demonstrated the expected deprotonated molecular ion and nitrate adducts, respectively. In addition, we demonstrated material consumption by investigating the analyte signal decay as a function of time.

TNT

A 1 µg of sample was pipetted onto a Prosolia sample slide and sampled at the specified potential for, and averaged over, 30 s by a 50 % (volume fraction) methanol/water at a flow rate of 3.5 µL/min and focused gas pressure of (70 ± 14) kPa. Figure S4 displays a representative mass spectra of TNT, demonstrating the deprotonated ion $[M\text{-}H]^-$ at *m/z* 226.

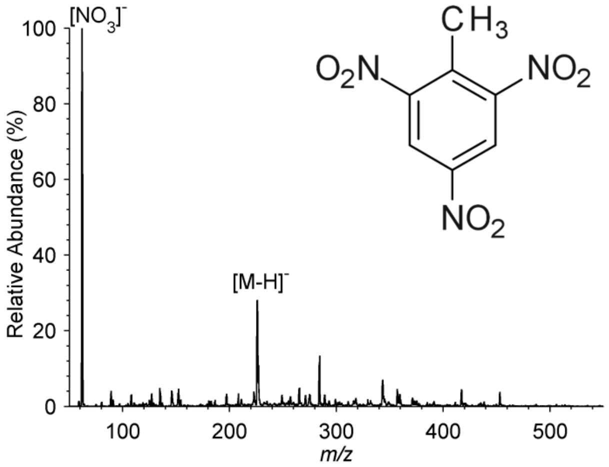

Figure S4. Negative ion mode DEFFI mass spectrum of 1 µg of TNT placed on a standard Prosolia sample slide and sampled for 30 s at -250 V. Inset: TNT chemical structure.

RDX

We investigated the analyte signal decay as a function of time utilizing inkjet printing of explosive standards onto the samples spot of a Prosolia sample slide. Successive individual drops were inkjet printed until 5 ng of material was deposited. Each spot was sampled for 10 minutes by a 50 % (volume fraction) methanol/water at a flow rate of 3.5 µL/min, focused gas pressure of (70 ± 14) kPa, and -250 V applied potential. Figure S5 displays the total ion chromatogram (TIC) and extracted ion chromatograms (XIC) for the nitrate, RDX monomer nitrate adduct, and RDX dimer nitrate adduct. The inset displays the expanded XICs for the RDX adducts, demonstrating the same signal decay observed for the TIC as the sample material was consumed.

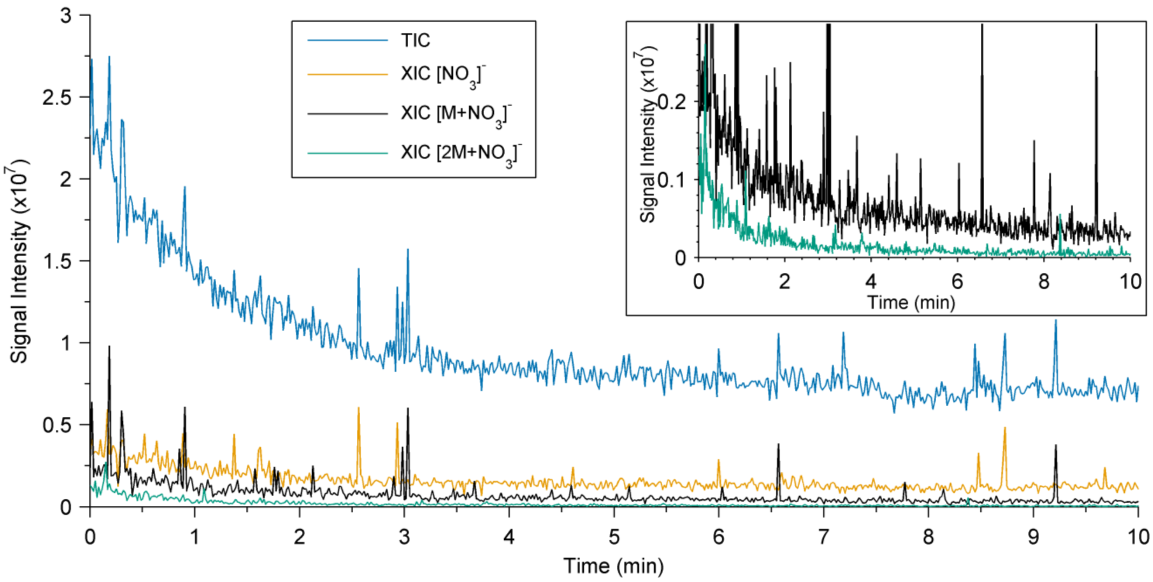

Figure S5. Negative ion mode DEFFI total ion chromatogram (TIC) and extracted ion chromatograms (XIC) for the nitrate, RDX monomer nitrate adduct, and RDX dimer nitrate adduct, of 5 ng of RDX placed on a standard Prosolia sample slide and sampled for 10 minutes at -250 V. Inset: Expanded extracted ion chromatograms for RDX monomer and dimer nitrate adducts.

Figure S6 displays the mass spectra for the 5 ng RDX sample from Figure S5. Similar to the representative RDX spectra displayed in the article text, the spectrum consisted of prominent peaks for the RDX monomer nitrate adduct at *m/z* 284 $[M+NO_3]^-$, the RDX dimer nitrate adduct at *m/z* 506 $[2M+NO_3]^-$, and nitrate at *m/z* 62 $[NO_3]^-$.

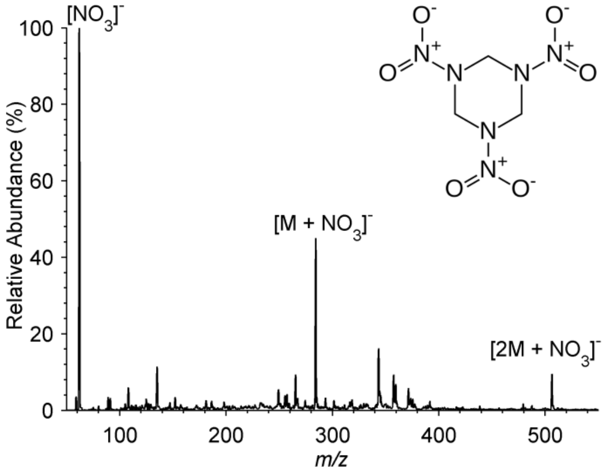

Figure S6. Negative ion mode DEFFI mass spectrum of 5 ng of RDX placed on a standard Prosolia sample slide and sampled for 10 minutes at -250 V. Inset: RDX chemical structure.

PETN

The signal decay as a function of time was also investigated for PETN utilizing inkjet printing onto the samples spot of a Prosolia sample slide. Each spot, containing 5 ng PETN, was sampled for 10 minutes by a 50 % (volume fraction) methanol/water at a flow rate of 3.5 µL/min, focused gas pressure of (70 ± 14) kPa, and -250 V applied potential. Similar to RDX, Figure S7 displays the total ion chromatogram (TIC) and extracted ion chromatograms (XIC) for the nitrate and PETN nitrate adduct. The inset displays the expanded XIC for the PETN nitrate adduct, clearly demonstrating material consumption.

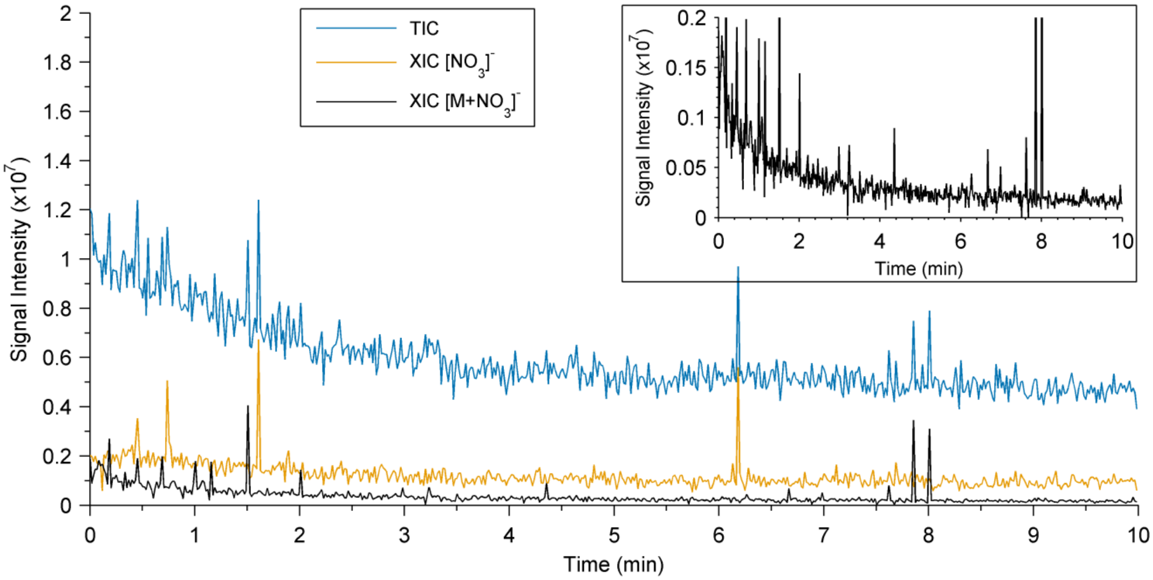

Figure S7. Negative ion mode DEFFI total ion chromatogram (TIC) and extracted ion chromatograms (XIC) for the nitrate and PETN monomer nitrate adduct, of 5 ng of PETN placed on a standard Prosolia sample slide and sampled for 10 minutes at -250 V. Inset: Expanded extracted ion chromatogram for PETN nitrate adduct.

Finally, we provide the PETN mass spectra for 5 ng sampled for 10 minutes. Prominent peaks for the PETN nitrate adduct at *m/z* 378 [M+NO$_3$]$^-$ and nitrate at *m/z* 62 [NO$_3$]$^-$, as well as PETN's chemical structure are displayed in Figure S8.

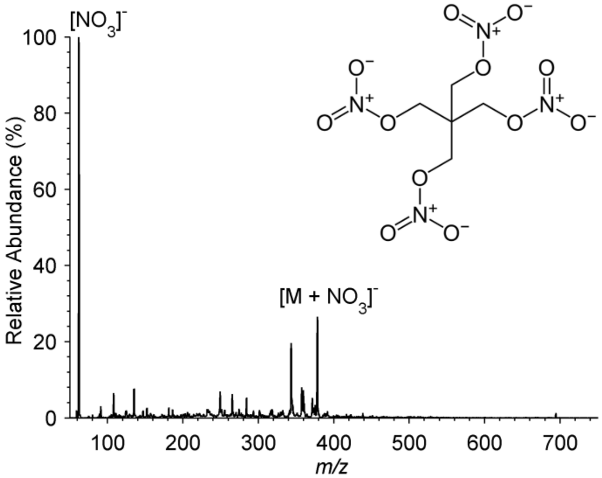

Figure S8. Negative ion mode DEFFI mass spectrum of 5 ng of PETN placed on a standard Prosolia sample slide and sampled for 10 minutes at -250 V. Inset: PETN chemical structure.

References

1. M. Volny, A. Venter, S. A. Smith, M. Pazzi and R. G. Cooks, *Analyst*, 2008, **133**, 525-531.
2. T. P. Forbes, T. M. Brewer and G. Gillen, *Applied Physics Letters*, 2013, **102**, 214102-214104.
3. K. Douglass, S. Jain, W. Brandt and A. Venter, *Journal of The American Society for Mass Spectrometry*, 2012, **23**, 1896-1902.